Virus Labeling

DOI: 10.1002/anie.201105701

Multicolor Labeling of Living-Virus Particles in Live Cells**

Peng Zhou, Zhenhua Zheng, Wen Lu, Fuxian Zhang, Zhenfeng Zhang, Daiwen Pang, Bin Hu, Zhike He, and Hanzhong Wang**

Tracking living viruses in host cells is of great importance for the understanding of viral infections and developing therapies for viral diseases. The viral infection of host cells is a highly dynamic process composed of multiple steps. For instance, the enveloped virus initiates the infection by membrane fusion between the viral envelope and the cell membrane. The viral genomes are subsequently released in endosomes and then transported into the nucleus; finally, the expression of viral genes occurs. The loss of the viral envelope and release of viral genomes are the hallmarks of enveloped-virus infection events,[1–4] and the real-time tracking of these critical events in viral infection has been considered highly important to the better understanding of the viral infection mechanisms. In past decades, two general strategies have been developed for labeling viruses: fusion of a target viral protein with a fluorescent protein (FP) or direct chemical labeling of an external viral protein with fluorescent probes. These labeling approaches have provided important insights into the transport and uncoating mechanisms of viruses. However, these approaches cannot be applied to track the release of the viral genome after membrane fusion, thus resulting in the loss of critical information about late infection events after membrane fusion.[5–7] Thus, the labeling and tracking of different viral components, particularly of the viral genome during a viral infection, are needed for the complete understanding of viral infection mechanisms. Unfortunately, owing to the inaccessibility of the viral genome after the completion of the viral assembly and the lack of an ideal nucleic acid probe, viral-genome labeling has always been a challenge. Meanwhile, the labeling of the viral genome is also the current bottleneck of studies on tracking of the complete virus infection process.

Herein, we describe a new strategy for synchronous multicolor labeling of a living virus in live cells. The viral genomes were labeled by using an in vivo virus self-assembly system in combination with a novel nucleic acid probe based on a ruthenium complex, and the viral envelope was labeled by fusing a characteristic external viral protein with green fluorescent protein (GFP). Multicolor labeling of distinct viral components can be done during the viral replication in host cells (Scheme 1). More importantly, labeling a virus in this manner can overcome the photobleaching and self-quenching effects between dye molecules and does not affect the viral infectivity.

In recent years, the molecular light-switch metal complexes of dppz, such as $[Ru(phen)_2(dppz)]^{2+}$, have been frequently used in cellular imaging studies,[8–14] owing to their strong binding to double-stranded DNA, low background emission, and the extraordinary photophysical properties of their long-lived excited metal-to-ligand charge-transfer state and the red-shifted emission. Furthermore, their organic ligands can be readily modified to tune the selectivity and reactivity of the complex for a particular disease target, thereby making the metal complexes widely applicable therapeutic agents for the treatment of cancer, human

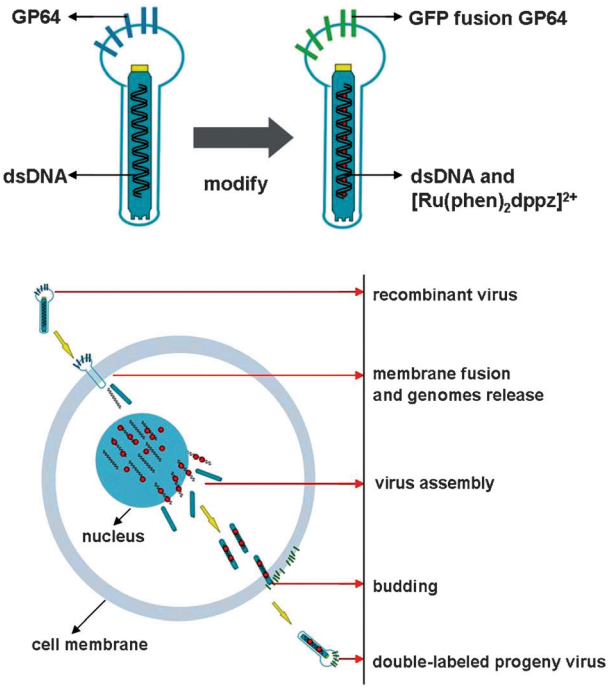

Scheme 1. Multicolor labeling of living-virus particles in live cells. dsDNA = double-stranded DNA, GP64 = glycoprotein 64 of baculoviruses, phen = 1,10-phenanthroline, dppz = dipyridophenazine.

[*] P. Zhou, W. Lu, Prof. D. Pang, Prof. B. Hu, Prof. Z. He
Key Laboratory of Analytical Chemistry for Biology and Medicine (Ministry of Education), College of Chemistry and Molecular Sciences, Wuhan University
Wuhan 430072 (P. R. China)
E-mail: zhkhe@whu.edu.cn
Z. Zheng, F. Zhang, Z. Zhang, Prof. H. Wang
State Key Laboratory of Virology, Wuhan Institute of Virology, Chinese Academy of Sciences
Xiaohongshan NO.44, Wuhan, 430071 (P. R. China)
E-mail: wanghz@wh.iov.cn

[**] This work was supported by the National Key Scientific Program-Nanoscience and Nanotechnology (2011CB933600), 973 Program (2007CB714507), the National Science Foundation of China (21075093, 20875071, 30770083) and the Science Fund for Creative Research Groups of NSFC (20921062).
Supporting information for this article is available on the WWW under http://dx.doi.org/10.1002/anie.201105701.

immunodeficiency virus, and Alzheimer's disease.[15–17] In this research, we extended the application of these ruthenium complexes to living-virus-genome labeling and to virus tracking. Baculoviruses, well-known enveloped viruses, were chosen as the model system for the living-virus-genome labeling study herein. These enveloped viruses contain large circular double-stranded DNA genomes ranging in size from 80 to 180 kbp, and their transcription, DNA replication, and nucleocapsid assembly occurs within the nuclei of infected cells.[15] To avoid having to label the viral genome after it becomes inaccessible, that is, after the completion of viral assembly, we labeled the viral genome with $[Ru(phen)_2(dppz)]^{2+}$ during the virus self-assembly process. To fluorescently label the external viral protein, the baculovirus's encoded glycoprotein GP64, which is the key structure protein for the membrane fusion of a virus infection,[18,19] was fused with GFP (Figure S1 in the Supporting Information). By monitoring the GFP expression level in host cells, we can categorize the viral infection process into different stages and thus obtain an approximate time measurement of the viral infection event. Furthermore, once the viral genomes were successfully labeled with $[Ru(phen)_2(dppz)]^{2+}$ during the viral replication, progeny virus particles generated in this system might finally contain a green fluorescent envelope and red fluorescent nucleic acid. Such multicolor labeling of distinct viral components allows the monitoring of viral disassembly during infection, which may provide the crucial dynamic information for a more complete understanding of viral infection mechanisms in vivo.

In the viral-genome labeling experiments, a systematic investigation including cellular uptake, intracellular distribution, and cytotoxicity analysis was first carried out to evaluate the influence of $[Ru(phen)_2(dppz)]^{2+}$ on the bioactivity of the host cells (*Spodoptera frugiperda* Sf9). Cellular uptake experiments revealed that above the concentration threshold of 10 μM, the cellular uptake of $[Ru(phen)_2(dppz)]^{2+}$ increases dramatically up to the concentration of 20 μM (data not shown). Confocal microscopy imaging confirmed that the luminescence was distributed throughout the cytoplasm, though mostly excluded from the nucleus (Figure 1). Cytotoxicity analysis and counting of dead cells indicated that even at a high concentration of 20 μM Sf9 cells still maintained the normal morphology and proliferation during the cell growth cycle, and no apparent cytotoxicity or dead cells were observed compared with the control.

Virus-infected cells have diverse morphologies compared with uninfected cells. We also evaluated the influence of a virus infection on the cellular uptake of $[Ru(phen)_2(dppz)]^{2+}$ in host cells. The $[Ru(phen)_2(dppz)]^{2+}$ was added into the host cells at the same time as the virus. The cellular uptake of $[Ru(phen)_2(dppz)]^{2+}$ in infected cells could be clearly divided into two phases (Figure 2a, b). In the first phase, no apparent cellular pathological changes were observed. The cellular uptake level and intracellular distribution of $[Ru(phen)_2(dppz)]^{2+}$ in the infected cells were the same as in the uninfected cells. The absence of green fluorescence in host cells indicated that this phase corresponds to the viral incubation period, in which no progeny virus particles were generated (0 h, Figure 2a). In the second phase, the emergence of green fluorescence in host cells indicated that this phase was the viral infection medium-term, in which the initial progeny virus particles were generated. Many pathological changes were observed in the infected cell, such as the expansion of cells and damage of membrane integrity (Figure S2 in the Supporting Information), which was due to the budding of initial progeny virus particles, resulting in the dramatically increased cellular uptake level of $[Ru(phen)_2(dppz)]^{2+}$ in cells and the elevated accumulation of luminescence in the nucleus. In this case, both the host cells' genomes and progeny viruses' genomes can be simultaneously labeled with $[Ru(phen)_2(dppz)]^{2+}$ during the viral replication. Co-localization analysis of $[Ru(phen)_2(dppz)]^{2+}$ and GFP in infected cells showed that starting with the viral infection medium-term (48 h Figure 2a) the fluorescence of both colors gradually increased throughout the infected cells. The increase lasted to the late stage of virus infection, when at least 80% of the cells had the apparent co-localization of two colors of fluorescence (144 h, Figure 2a), suggesting that the gradual accumulation of $[Ru(phen)_2(dppz)]^{2+}$ in the nucleus (Figure S3 the Supporting Information) does not affect the generation of progeny viruses. This result ensures that the labeled virus genomes can be packaged into the progeny virus particles by the in vivo viral self-assembly system.

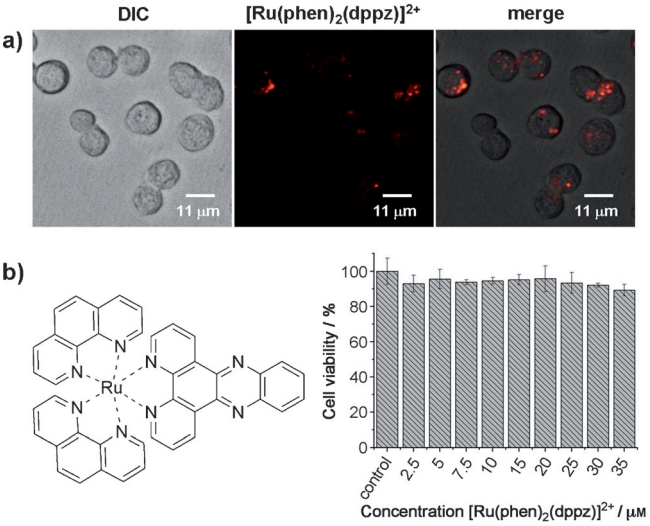

Figure 1. a) Cellular uptake and subcellular distribution of ruthenium complexes. Sf9 cells were incubated with 20 μM $[Ru(phen)_2(dppz)]^{2+}$ for 24 h at 28 °C in complete medium and then imaged by confocal microscopy. Differential interference contrast (DIC) and fluorescence microscopy image of Sf9 cells showed that the punctate staining of ruthenium was distributed throughout the cytoplasm but mostly excluded from the nucleus. b) Structure of $[Ru(phen)_2(dppz)]^{2+}$ (left). Cytotoxicity analysis (Cell Counting Kit-8) of Sf9 cells incubated with $[Ru(phen)_2(dppz)]^{2+}$ at different concentrations (right).

According to the virus titer calculation and ICP-MS measurements on the purified progeny virus, we found that the tissue culture infective dose ($TCID_{50}$) of purified progeny virus solution was $3.5 \times 10^8\ mL^{-1}$and the concentration of $[Ru(phen)_2(dppz)]^{2+}$ in progeny virus supernatants was 74 μM. That means that one living-virus particle contained approximately 2.1×10^{-7} nmol $[Ru(phen)_2(dppz)]^{2+}$. Obviously, besides labeling the viral genomes, excessive $[Ru(phen)_2$-

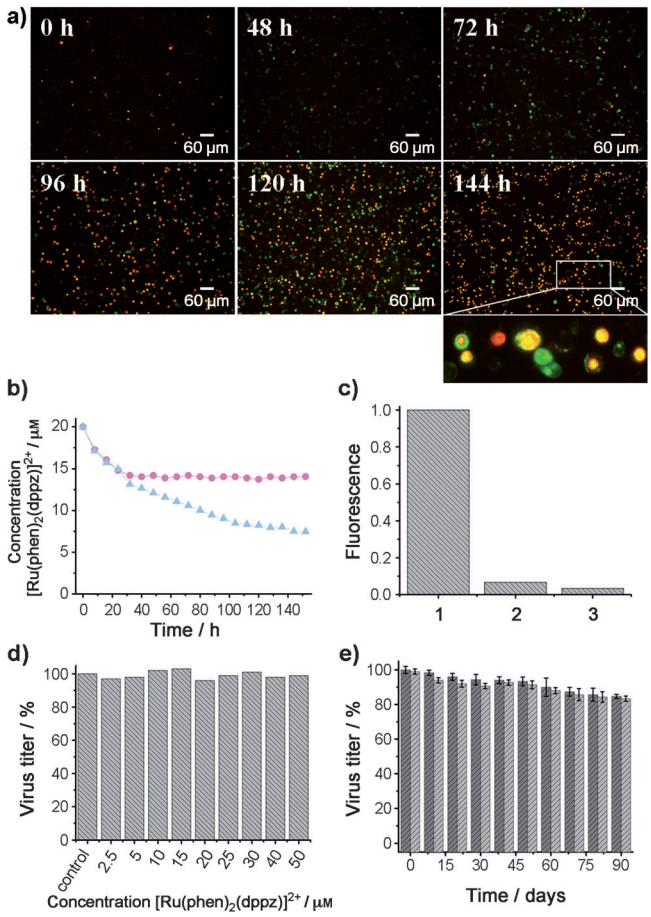

Figure 2. Effect of virus infection on cellular uptake of $[Ru(phen)_2(dppz)]^{2+}$ in host cells. a) Time-lapse confocal microscopy images of baculoviruses in Sf9 cells in the presence of 20 μM $[Ru(phen)_2(dppz)]^{2+}$. Red $[Ru(phen)_2(dppz)]^{2+}$, green GFP, yellow colocalization of red and green fluorescence. b) Time-lapse inductively coupled plasma mass spectrometry (ICP-MS) measurements of $[Ru(phen)_2(dppz)]^{2+}$ concentration in the supernatant of Sf9 cells with (blue triangle) or without virus infection (purple circle). c) Fluorescence measurements of $[Ru(phen)_2(dppz)]^{2+}$ in progeny virus supernatants with (1) and without (2) protein degradation by protease K. The control (3) was 10 mM pH 7.0 sodium phosphate solution. d) Effect of initial $[Ru(phen)_2(dppz)]^{2+}$ concentrations on the infectivity of progeny virus particles. e) The viral infectivity attenuation of wild-type viruses (dark gray) and labeled viruses (light gray) within three months preservation at 4 °C.

$(dppz)]^{2+}$ had been packaged into the progeny virus particles during the viral replication. The excess of $[Ru(phen)_2(dppz)]^{2+}$ inside the virus particles could ensure a high labeling efficiency of the progeny viral genome and provide a stable fluorescence signal in the real-time tracking of virus particles in live cells. To address the question of whether the $[Ru(phen)_2(dppz)]^{2+}$ fluorescence indeed originated from the inside of viruses, viral protein degradation by protease K was performed. Progeny virus supernatants were obtained by salting out either directly from the progeny virus solution or after protein degradation by protease K. A comparison of the fluorescence spectra of the two supernatants (Figure 2c) showed that without the degradation of external viral protein, the $[Ru(phen)_2(dppz)]^{2+}$ fluorescence signal could hardly be detected in the progeny virus supernatants, thus suggesting that almost all of the $[Ru(phen)_2(dppz)]^{2+}$ fluorescence was exclusively inside the virus particles rather than exposed on the viral surface; the location of fluorescence inside the particles originated from the binding between viral genomes and $[Ru(phen)_2(dppz)]^{2+}$.

As we indicated, the main viral-genome labeling during viral replication was due to the dramatic increase of $[Ru(phen)_2(dppz)]^{2+}$ concentration in the infected cells, which resulted from the cellular membrane damage. Therefore, the initial $[Ru(phen)_2(dppz)]^{2+}$ concentration in virus infection was critical to the packing efficiency of $[Ru(phen)_2(dppz)]^{2+}$ into the progeny virus particles. For the initial progeny virus particles that were generated before cellular membrane damage, the concentration should be higher than the concentration threshold of 10 μM. In this case, the $[Ru(phen)_2(dppz)]^{2+}$ could distribute throughout the cytoplasm and label the initial progeny virus particles during viral replication. Furthermore, for those rapid multiplicative viruses that were generated after cellular membrane damage, such high concentration of $[Ru(phen)_2(dppz)]^{2+}$ was crucial to the dramatic increase of the concentration of the metal complex in the infected cells. Under the same conditions, the initial time span before the $[Ru(phen)_2(dppz)]^{2+}$ concentration in the infected cells dramatically increased was observed to depend on the initial concentration. In this system, a $[Ru(phen)_2(dppz)]^{2+}$ concentration of 20 μM was chosen as the initial concentration in virus infection. As shown in Figure 2d,e, this high concentration of $[Ru(phen)_2(dppz)]^{2+}$ in viral infection did not affect the infectivity of progeny virus particles; even after preservation at 4 °C for three months, the labeled virus still had equivalent infectivity to the wild-type viruses.

Figure 3 shows the characterization of the purified progeny virus particles. At least 90% of virus particles were labeled with both $[Ru(phen)_2(dppz)]^{2+}$ and GFP and maintained the intact viral structure. In the subsequent research on tracking the infection with doubly labeled virus particles in host cells, fresh Sf9 cells with a cell density of $1\times10^6\,mL^{-1}$ were incubated with the progeny virus particle at 25 multiplicity of infection (MOI) under conditions that permit endocytosis of viruses. Time-lapse confocal microscopy images (Figure 4) showed both punctuate red fluorescence and green fluorescence localized exclusively at the cell surface at 4 °C. When the temperature shifted from 4 to 25 °C, apparent separation between the two kinds of fluorescence in cells was observed after 10 min. Rapid accumulation of red fluorescence in the cell nucleus and visible enrichment of green fluorescence in the cell membrane region were efficiently synchronized in this manner. Obviously, such distinct cellular location and transfer of the two kinds of fluorescence resulted from the viral infection in host cells. The virus fusion and release of viral genomes in host cells was a rapid and temperature-dependent event, which is consistent with previous virology studies.[20–22] More importantly, in our work this process has been excellently represented by the real-time tracking of the infection of live cells with doubly labeled viruses.

The four points listed below further demonstrate that the viral genomes were labeled with $[Ru(phen)_2(dppz)]^{2+}$. First,

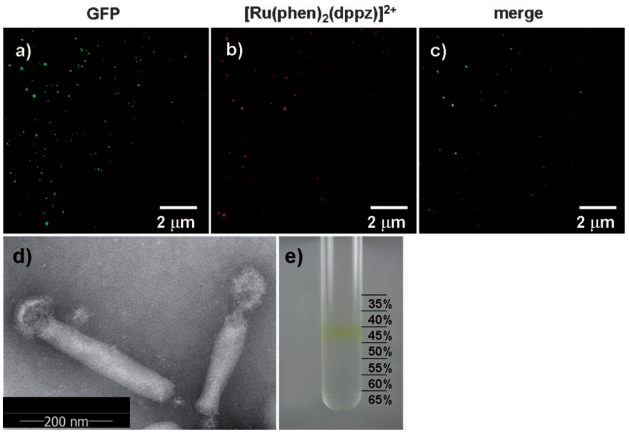

Figure 3. Characterization and purification of doubly labeled virus particles. a–c) Confocal microscopy images of progeny virus particles. d) TEM images of progeny virus particles. e) Image of a sucrose density gradient centrifugation (SDGC) tube after the separation of progeny virus particles. Fraction 45% was the major fluorescent band in the SDGC tube.

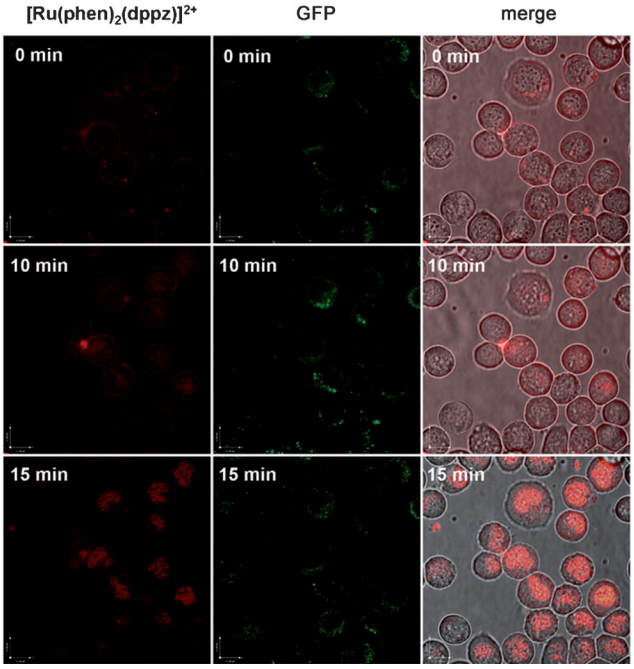

Figure 4. Time-lapse images of doubly labeled virus particles in host cells at 25 °C. Fresh Sf9 cells were infected with the progeny virus at 25 MOI. The viral infection was synchronized by incubating progeny virus and Sf9 cells at 4 °C and then raising the temperature to 25 °C to permit endocytosis of virus.

in the progeny viral infection all of the $[Ru(phen)_2(dppz)]^{2+}$ originated from the progeny viruses. The final concentration of $[Ru(phen)_2(dppz)]^{2+}$ in the supernatant of Sf9 cells had been measured to be lower than five micromolar. Such low amounts of $[Ru(phen)_2(dppz)]^{2+}$ could not enter into the cell nucleus and be imaged by microscopy, unless the $[Ru(phen)_2(dppz)]^{2+}$ was encapsulated into the viruses and protected by viral genomes. Second, no morphology change and membrane damage of the host cell occurred in the brief infection process, which could exclude the possibility of accumulation of excess $[Ru(phen)_2(dppz)]^{2+}$ in the nucleus owing to cell pathological change. Third, the trafficking of $[Ru(phen)_2(dppz)]^{2+}$ and GFP luminescence in host cells was rapid and temperature-dependent, which was highly consistent with the early studies on membrane fusion of baculoviruses infection. Fourth, the negative control experiment with *Heliothis Zea* (HZ) cells (HZ cells were nonpermissive to baculoviruses infection) confirmed that the moving of $[Ru(phen)_2(dppz)]^{2+}$ fluorescence into the nucleus was specific to the viral host cells (Figure S4 in the Supporting Information).[23]

Taken together, these results established that the viral genomes were indeed labeled with the ruthenium complexes. To our knowledge, this is the first time that ruthenium complexes were used for the labeling of living-virus particles. Also the strategy of viral-genome labeling by using this in vivo viral self-assembly system is rarely reported. Labeling viral genomes in this manner results in an excellent fluorescence signal in cellular imaging and does not affect the viral infectivity. Through the real-time tracking of doubly labeled virus particles in live cells, more information about the virus fusion with host cells and viral-genome trafficking in the nucleus has been obtained by fluorescence measurements. This information is crucial for the understanding of viral infection mechanisms. We hope that our method could serve as a new platform for the further study of viral infection mechanisms and also be used for other viruses, such as ssDNA or ssRNA viruses that have multiple palindromic structures.

Experimental Section

Cells and viruses and recombinant virus construction: *Spodoptera frugiperda* (Sf9) cells and *Heliothis Zea* (Hz cells) were propagated at 28 °C in Grace's insect medium (Gibco-BRL) supplemented with 10% fetal bovine serum (FBS, Gibco-BRL), pH 6.0. *Autographa californica* nucleopolyhedrovirus (AcMNPV), a typical baculovirus, was chosen as the model system for the living-virus genome study. The viruses were produced in Sf9 cells grown in Grace's insect medium (Gibco-BRL) supplemented with 10% fetal bovine serum (FBS, Gibco-BRL) at 25 °C pH 6.0. The recombinant AcMNPV, displaying enhanced green fluorescent protein (EGFP), vAc-EGFP-GP64 (Figure S1 in the Supporting Information), was generated according to the manufacturer's instructions for the Bac-to-Bac baculovirus expression system (Invitrogen). To generate the donor plasmid pFB-EGFP/GP64, the EGFP cassette was amplified from the pEGFP-N1 plasmid (Clontech) and its N terminus was fused with the GP64 signal peptide and the C terminus was fused with the GP64 mature peptide by PCR. The PCR product was digested with EcoRI and HindIII and subcloned downstream of the pPH promoter of the transfer vector pFastBac1 (Invitrogen). The recombinant AcMNPV virus was generated by transposition according to the manual of the Bac-to-Bac baculovirus expression system (Invitrogen).

Purification of progeny virus: Supernatants from virus-infected cell were harvested at day 5. The harvested supernatants were subjected to centrifugation at 5000 g for 30 min at 4 °C and then filtered through filters with a poresize of 0.45 μm. The viruses were pelleted by centrifugation at 100000 g for 4 h at 4 °C in a Beckman (Fullerton, CA) SW 28 rotor. The pellet was resuspended in 10 mM phosphate-buffered saline (PBS), pH 7.0. The suspension was loaded onto a sucrose density gradient (1 mL 65%, 1 mL 60%, 1 mL 55%,

1 mL 50%, 1 mL 45%, 1 mL 40%, 1 mL 35%, 1 mL 30%, 1 mL 25%, 1 mL 20%, 1 mL 15%) and centrifuged at 120000 g for 3 h at 4 °C; fraction 45% was the major fluorescent band in the SDGC tube. This band was collected and stored in 1 mL 10 mM PBS pH 7.0.

Fluorescence assays: For the fluorescence assay, the resuspended progeny virus solution was incubated with protease K (10 mg mL^{-1}) at 55 °C for 12 h, and then the supernatants were separated through the protein salting-out effect[24] and centrifugation at 10000 g for 20 min at 4 °C. Aliquots (100 μL) of supernatant were diluted with sodium phosphate buffer (1 mL, 10 mM, pH 7.0) and shaken a few times before their fluorescence emission was measured on a fluorometer (PerkinElmer LS55) at ambient temperature. The excitation wavelength was 400 nm, and the emission was recorded at 600 nm.

Transmission electron microscopy: For TEM examination, a sample (10 μL) was dropped onto a carbon-coated copper grid, removed after 2 min with filter paper, and left unstained or negatively stained. For negative staining, phosphotungstate (1%, 10 μL) was applied to the sample-loaded grid and blotted off after 20 minutes. The samples were observed with a Hitachi H7000 electron microscope. The software Image J (NIH) was used for the TEM image processing and data analysis.

Viral titration: The titers of supernatants were determined by an end-point dilution assay (EPDA) on Sf9 cells, and the final results were checked 7 days after the EPDA.

Metal complex synthesis and preparation of solutions: The synthesis of $[Ru(phen)_2(dppz)]^{2+}$ was performed according to previous reports.[25] A stock solution containing $[Ru(phen)_2(dppz)]^{2+}$ (10^{-4} mol L^{-1}) in ultrapure water was prepared and filtered through filters with a pore size of 0.22 μm prior to each experiment.

ICP-MS detection of Ru: The supernatant of Sf9 cells was isolated by centrifugation and then digested in a solution containing concentrated nitric acid and H_2O_2 (3:1) for 4 h at 90 °C, finally diluted 10-fold with Millipore water to 1.0 mL for Ru measurement. The Ru content was measured using Agilent 7500 series ICP-MS.

Fluorescence microscopy: Confocal laser scanning microscopy was performed with a PerkinElmer UltraView VOX system using a Nikon Ti microscope with 60×, 40×, and 20× objectives. GFP and $[Ru(phen)_2(dppz)]^{2+}$ were excited at a laser wavelength of 488 nm. Fluorescence emission was detected using a 525 nm band-pass filter for GFP. $[Ru(phen)_2(dppz)]^{2+}$ fluorescence was detected using long-pass filters of 605 nm. Live-cell imaging was performed with cells growing in 35 mm cell culture dishes. Cells were seeded at a density of 1×10^6 cells per milliliter. During acquisition, the cells were incubated in a heated chamber at 25 °C. Images were processed and analyzed using Andor Bioimaging software.

Received: August 12, 2011
Revised: October 12, 2011
Published online: December 1, 2011

Keywords: fluorescent probes · multicolor labeling · ruthenium · self-assembly · viruses

[1] D. M. Eckert, P. S. Kim, *Annu. Rev. Biochem.* **2001**, *70*, 777–810.
[2] L. Pelkmans, A. Helenius, *Curr. Opin. Cell Biol.* **2003**, *15*, 414–422.
[3] K. S. Matlin, H. Reggio, A. Helenius, K. Simons, *J. Cell Biol.* **1981**, *91*, 601–613.
[4] P. Wang, D. A. Hammer, R. R. Granados, *J. Gen. Virol.* **1997**, *78*, 3081–3089.
[5] B. Brandenburg, X. W. Zhuang, *Nat. Rev. Microbiol.* **2007**, *5*, 197–208.
[6] L. Pelkmans, J. Kartenbeck, A. Helenius, *Nat. Cell Biol.* **2001**, *3*, 473–483.
[7] K. M. Marks, G. P. Nolan, *Nat. Methods* **2006**, *3*, 591–596.
[8] C. A. Puckett, J. K. Barton, *Biochemistry* **2008**, *47*, 11711–11716.
[9] C. A. Puckett, R. J. Ernst, J. K. Barton, *Dalton Trans.* **2010**, *39*, 1159–1170.
[10] M. Matson, F. R. Svensson, B. Norden, P. Lincoln, *J. Phys. Chem. B* **2011**, *115*, 1706–1711.
[11] C. A. Puckett, J. K. Barton, *J. Am. Chem. Soc.* **2007**, *129*, 46–47.
[12] P. Nordell, F. Westerlund, L. M. Wilhelmsson, B. Nordén, P. Lincoln, *Angew. Chem.* **2007**, *119*, 2253–2256; *Angew. Chem. Int. Ed.* **2007**, *46*, 2203–2206.
[13] S. P. Foxon, T. Phillips, M. R. Gill, M. Towrie, A. W. Parker, M. Webb, J. A. Thomas, *Angew. Chem.* **2007**, *119*, 3760–3762; *Angew. Chem. Int. Ed.* **2007**, *46*, 3686–3688.
[14] S. Ji, W. Wu, W. Wu, H. Guo, J. Zhao, *Angew. Chem.* **2011**, *123*, 1664–1667; *Angew. Chem. Int. Ed.* **2011**, *50*, 1626–1629.
[15] D. L. Ma, C. M. Che, S. C. Yan, *J. Am. Chem. Soc.* **2009**, *131*, 1835–1846.
[16] B. Y. W. Man, H. M. Chan, C. H. Leung, D. S. H. Chan, L. P. Bai, Z. H. Jiang, H. W. Li, D. L. Ma, *Chem. Sci.* **2011**, *2*, 917–921.
[17] D. L. Ma, T. Xu, D. S. H. Chan, B. Y. W. Man, W. F. Fong, C. H. Leung, *Nucleic Acids Res.* **2011**, *39*, e67.
[18] B. M. Arif, *J. Invertebr. Pathol.* **2005**, *89*, 39–45.
[19] M. L. Wang, Y. Tan, F. F. Yin, F. Deng, J. M. Vlak, Z. H. Hu, H. L. Wang, *J. Virol.* **2008**, *82*, 9800–9804.
[20] K. L. Hefferon, A. G. P. Oomens, S. A. Monsma, C. M. Finnerty, G. W. Blissard, *Virology* **1999**, *258*, 455–468.
[21] N. D. van Loo, E. Fortunati, E. Ehlert, M. Rabelink, F. Grosveld, B. J. Scholte, *J. Virol.* **2001**, *75*, 961–970.
[22] G. W. Blissard, J. R. Wenz, *J. Virol.* **1992**, *66*, 6829–6835.
[23] H. J. R. Popham, J. J. Grasela, C. L. Goodman, A. H. McIntosh, *J. Insect Physiol.* **2010**, *56*, 1237–1245.
[24] T. Arakawa, S. N. Timasheff, *Biochemistry* **1984**, *23*, 5912–5923.
[25] E. Amouyal, A. Homsi, J. C. Chambron, J. P. Sauvage, *J. Chem. Soc. Dalton Trans.* **1990**, 1841–1845.

